ALFRED-WEGENER-INSTITUT
HELMHOLTZ-ZENTRUM FÜR POLAR- UND MEERESFORSCHUNG

JACOBS UNIVERSITY

TRR 181

MODELLING EDDIES IN GLOBAL EDDY-PERMITTING SIMULATIONS:

IMPACTS OF AN OCEAN KINETIC ENERGY BACKSCATTER PARAMETRIZATION

Stephan Juricke,
Sergey Danilov, Nikolay Koldunov,
Marcel Oliver, Dmitry Sidorenko

COMMODORE, Hamburg
31.01.2020

Sea surface
height variability

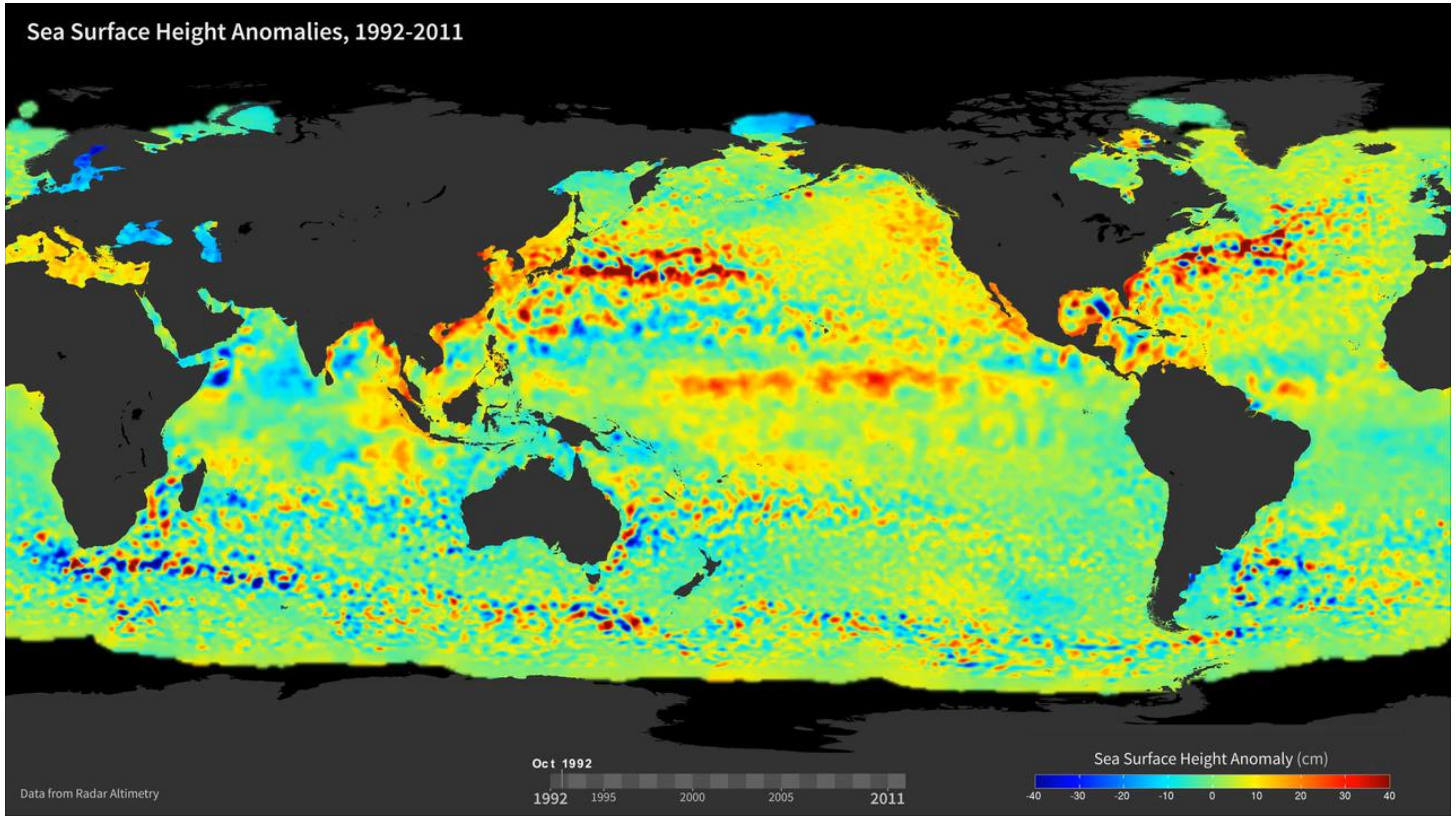

http://svs.gsfc.nasa.gov/cgi-bin/details.cgi?aid=30502

Sea surface height variability (AVISO relative to simulation)

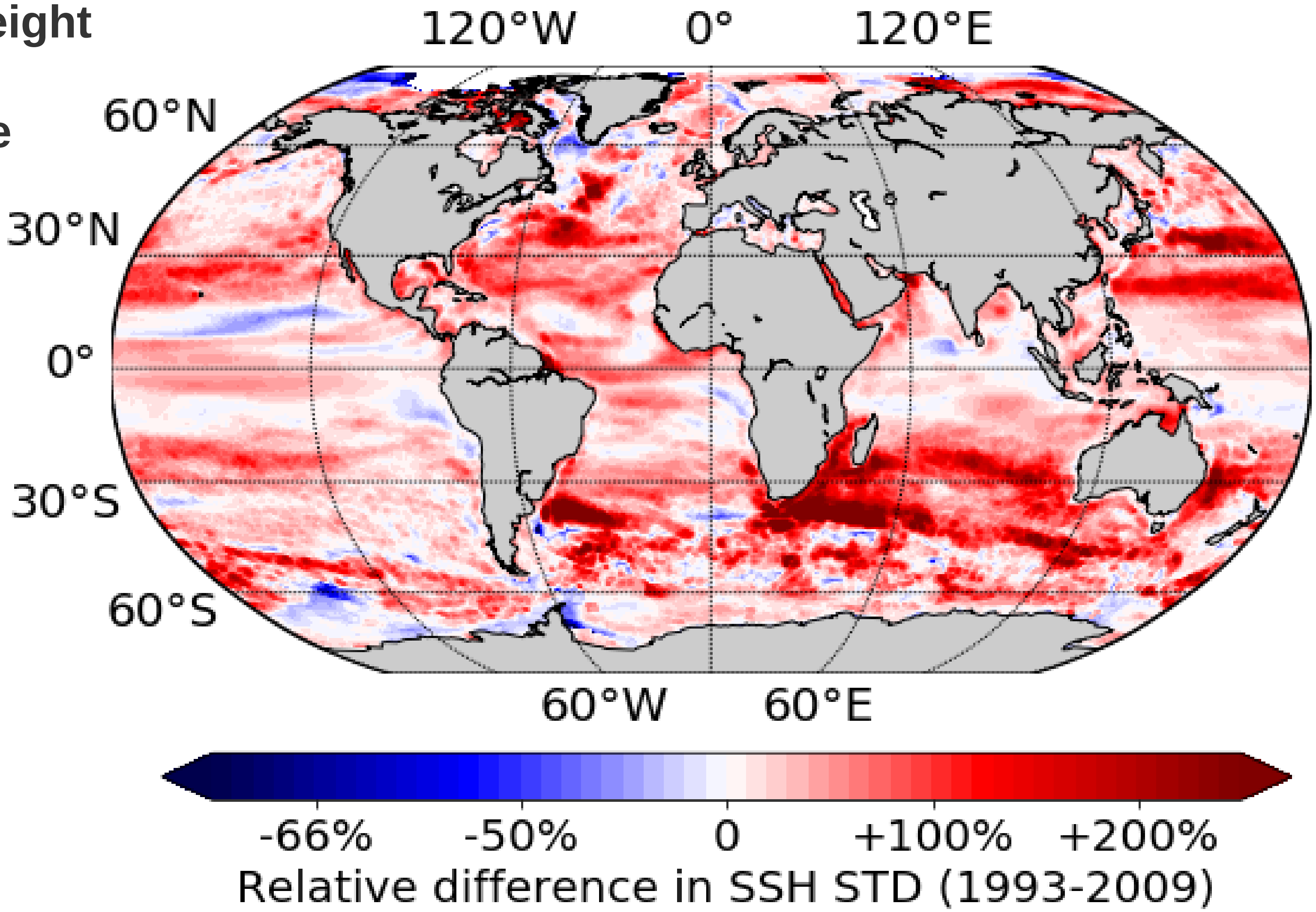

Strong underestimation by ¼° simulation when compared to AVISO observational estimates

No backscatter parametrization

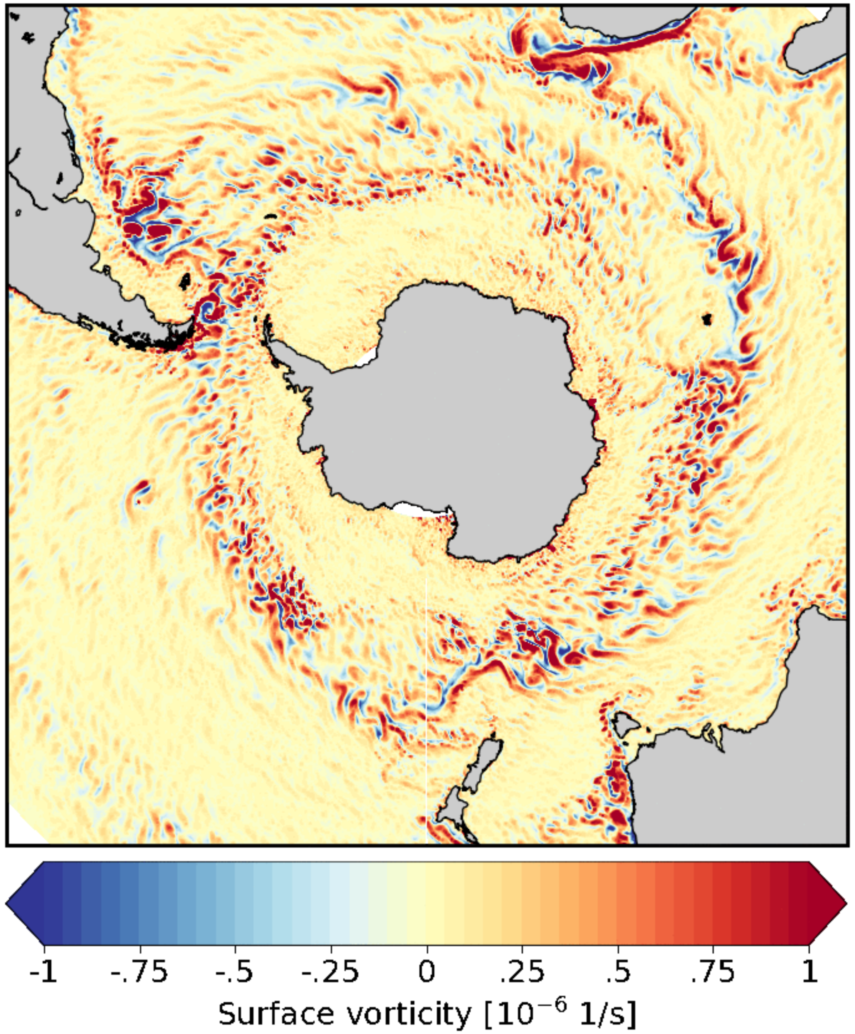

Eddy permitting FESOM2
1/4° global ocean simulation

Classical harmonic viscosity (modified harmonic Leith with biharmonic background)

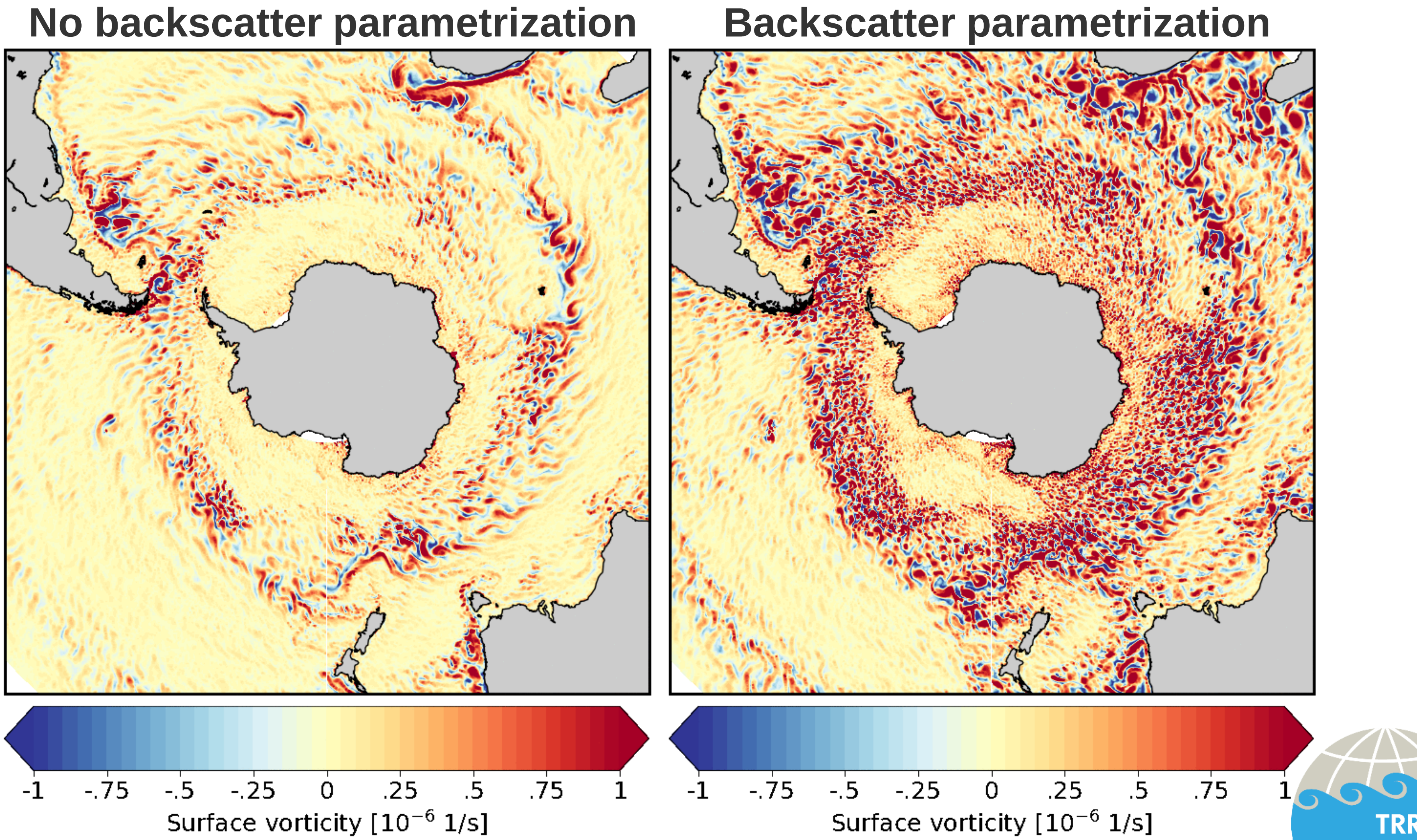
No backscatter parametrization
Backscatter parametrization
-1 -.75 -.5 -.25 0 .25 .5 .75 1
Surface vorticity [10^{-6} 1/s]
-1 -.75 -.5 -.25 0 .25 .5 .75 1
Surface vorticity [10^{-6} 1/s]

INTRODUCTION

In eddy-permitting ocean models only some of the largest eddies are explicitly simulated

Potential energy release by eddies through baroclinic instabilities is reduced

Missing eddy effects are essential for accurate simulations of the mean flow and variability

Viscosity closures dissipate not only enstrophy (i.e. vorticity variance; necessary for model stabilization) but also energy

Kinetic energy backscatter allows to (stably) reinject excessively dissipated energy into momentum equation

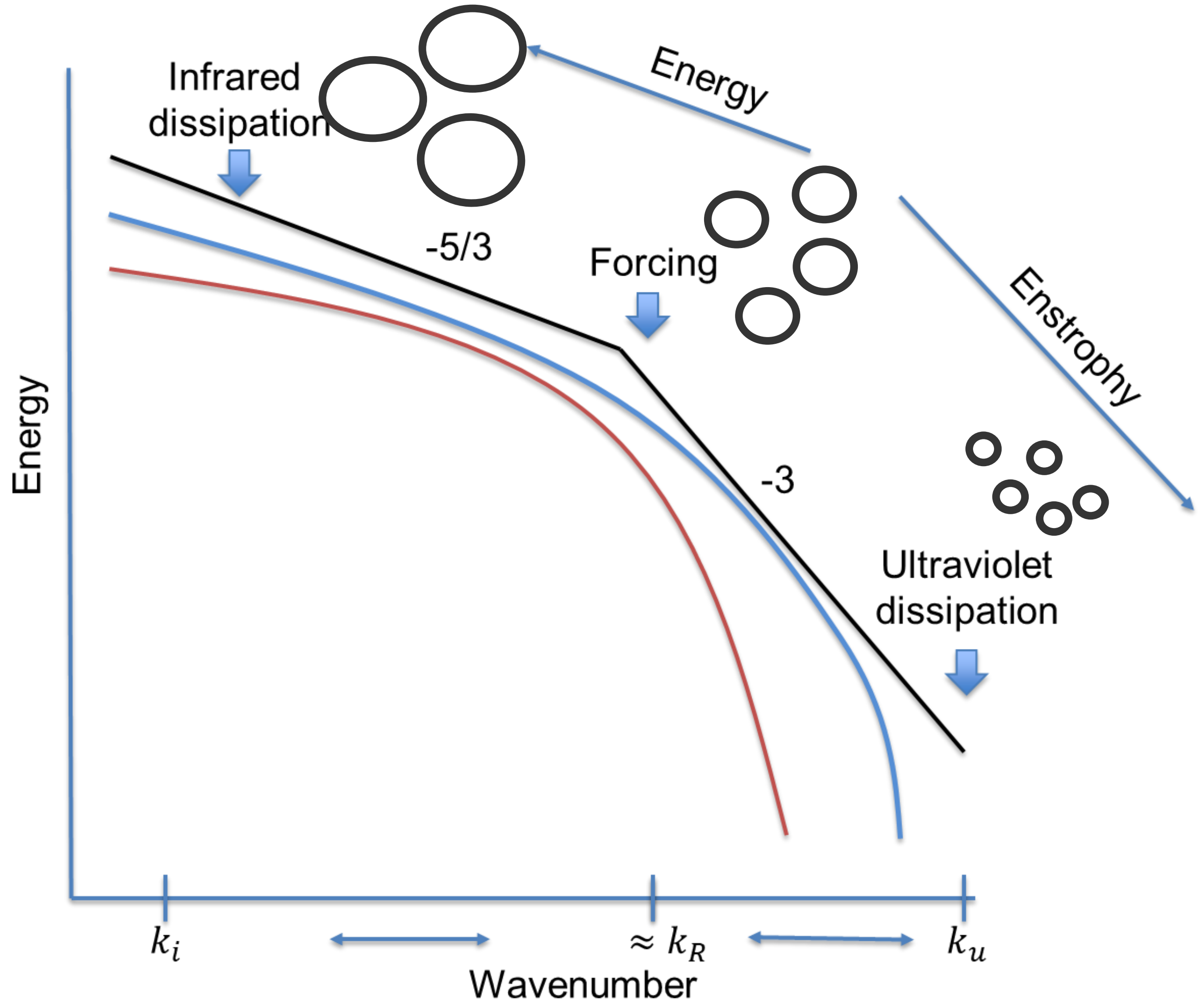
Infrared dissipation
Energy
-5/3
Forcing
Enstrophy
-3
Ultraviolet dissipation
Energy
k_i
$\approx k_R$
k_u
Wavenumber

Momentum equation with $\vec{v} = (\vec{u}, w)$:

dissipation at small scales

$$\vec{u}_t + \vec{u} \cdot \nabla \vec{u} + w \partial_z \vec{u} + f \vec{k} \times \vec{u} + \frac{1}{\rho_o} \nabla P = V(\vec{u}) + \qquad \partial_z (A_v \partial_z \vec{u})$$

$V(\vec{u})$ dissipation operator with flow-dependent coefficient (e.g. harmonic or biharmonic operator)

Momentum equation with $\vec{v} = (\vec{u}, w)$:

dissipation at small scales

$$\vec{u}_t + \vec{u} \cdot \nabla \vec{u} + w \partial_z \vec{u} + f \vec{k} \times \vec{u} + \frac{1}{\rho_o} \nabla P = V(\vec{u}) + B(\vec{u}) + \partial_z (A_v \partial_z \vec{u})$$

backscatter at larger scales

$V(\vec{u})$ dissipation operator with flow-dependent *positive* coefficient (e.g. harmonic or biharmonic operator)

$B(\vec{u})$ backscatter operator with flow-dependent *negative* coefficient (e.g. harmonic or smoothed harmonic operator)

Momentum equation with $\vec{v} = (\vec{u}, w)$:

Energy consistent operator

$$\vec{u}_t + \vec{u} \cdot \nabla \vec{u} + w \partial_z \vec{u} + f \vec{k} \times \vec{u} + \frac{1}{\rho_o} \nabla P = V(\vec{u}) + B(\vec{u}) + \partial_z (A_v \partial_z \vec{u})$$

$V(\vec{u})$ dissipation operator (small scales)
$B(\vec{u})$ backscatter operator (larger scales)

$V(\vec{u}) + B(\vec{u})$ dissipates energy and especially enstrophy (vorticity variance) at small scales, reinjects energy into larger scales to remain energetically consistent (as suggested by Jansen et al., 2015)

BACKSCATTER PARAMETRIZATION

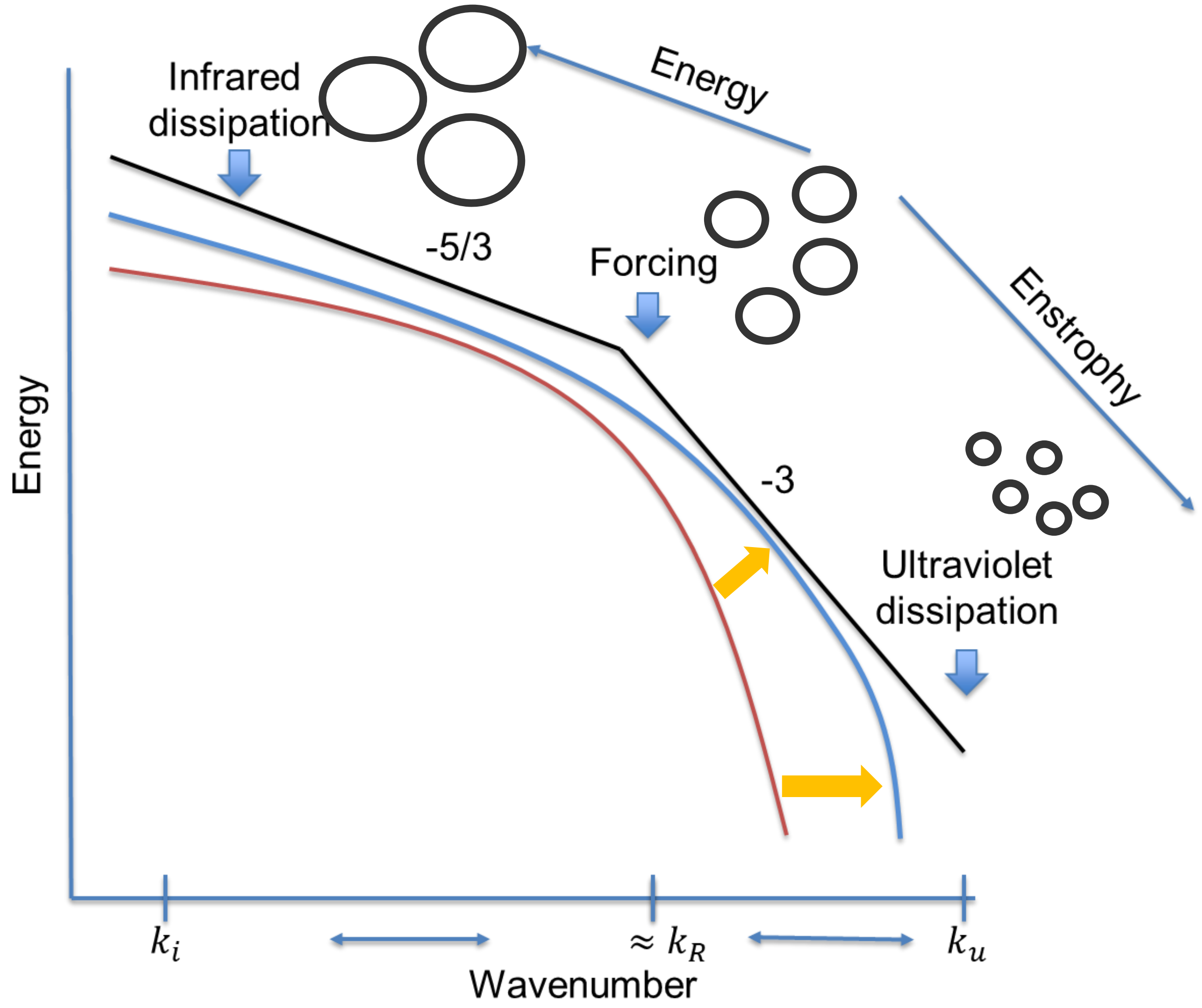

BACKSCATTER PARAMETRIZATION

$$\vec{u}_t + \vec{u} \cdot \nabla \vec{u} + w \partial_z \vec{u} + f\vec{k} \times \vec{u} + \frac{1}{\rho_o} \nabla P = V(\vec{u}) + B(\vec{u}) + \partial_z (A_v \partial_z \vec{u})$$

$(1 - c_{dis})\dot{E}_{dis}$

physical dissipation

Dissipation rate

Backscatter rate

$$\partial_t e = -c_{dis}\dot{E}_{dis} - \dot{E}_{back} + Diffusion$$

sub-grid kinetic energy $e(x, y, z, t)$

(Jansen et al., 2015; Klöwer et al., 2018)

Backscatter coefficient $\nu_b = -\boldsymbol{c_0 A}\sqrt{\mathbf{max}(\mathbf{2}\boldsymbol{e},\mathbf{0})}$

with scaling $\boldsymbol{c_0}$, grid spacing $\boldsymbol{A}$

sub-grid kinetic energy

Remark: Smoothing in time and space as a tool to separate dissipation from forcing scales → stabilization

Idealized model configuration

RESULTS: EQUIDISTANT CHANNEL

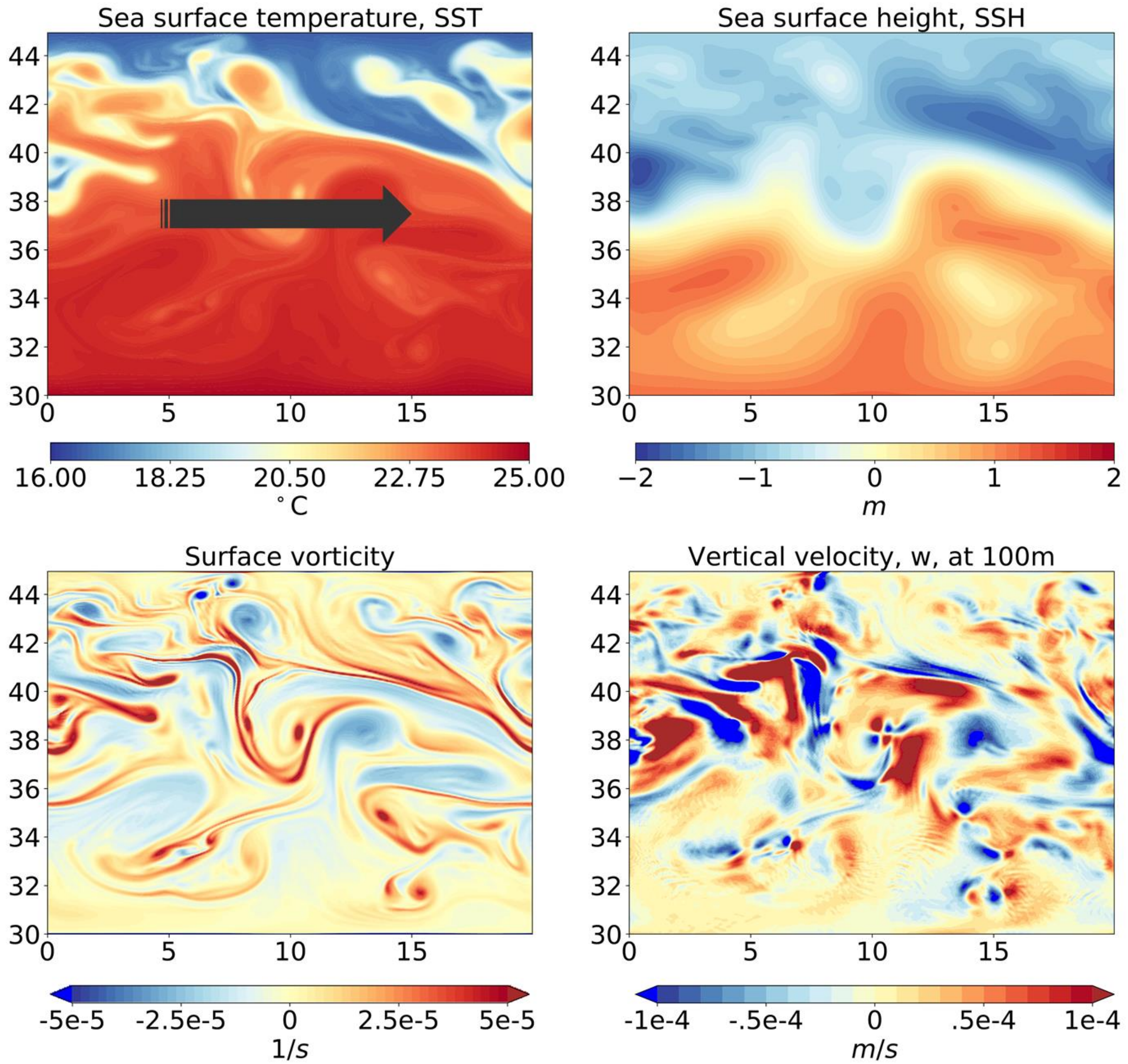

Zonally reentrant channel simulation (FESOM2)

1/12° resolution

24 vertical layers, 1600m depth

Equidistant grid configuration

Boundary temperature relaxation

10 years simulation length

Vertical structure (time mean layer averages)

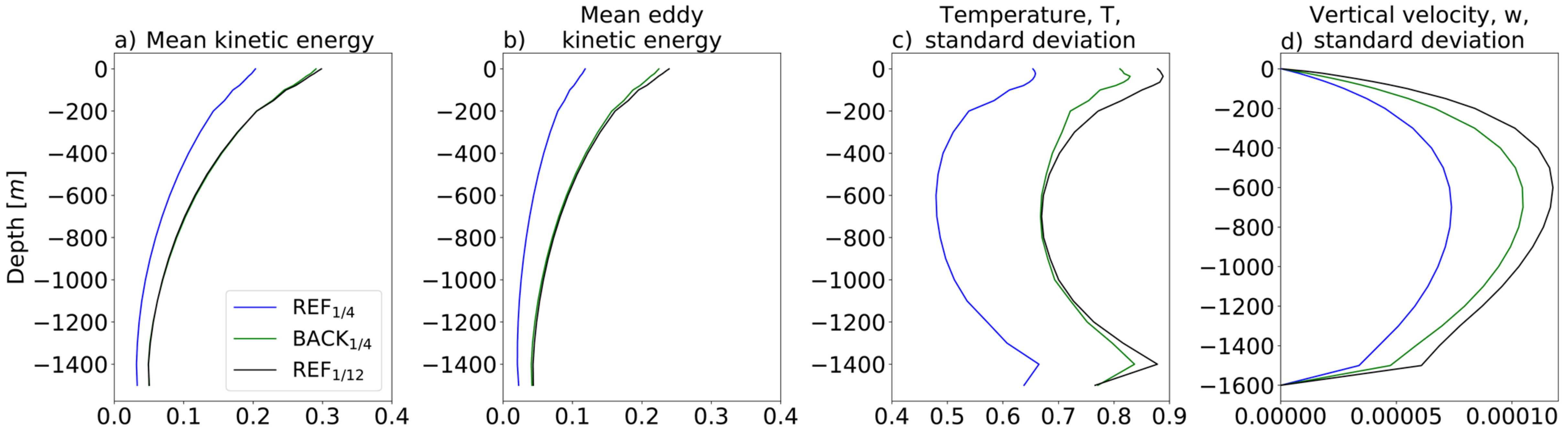

Global model configuration

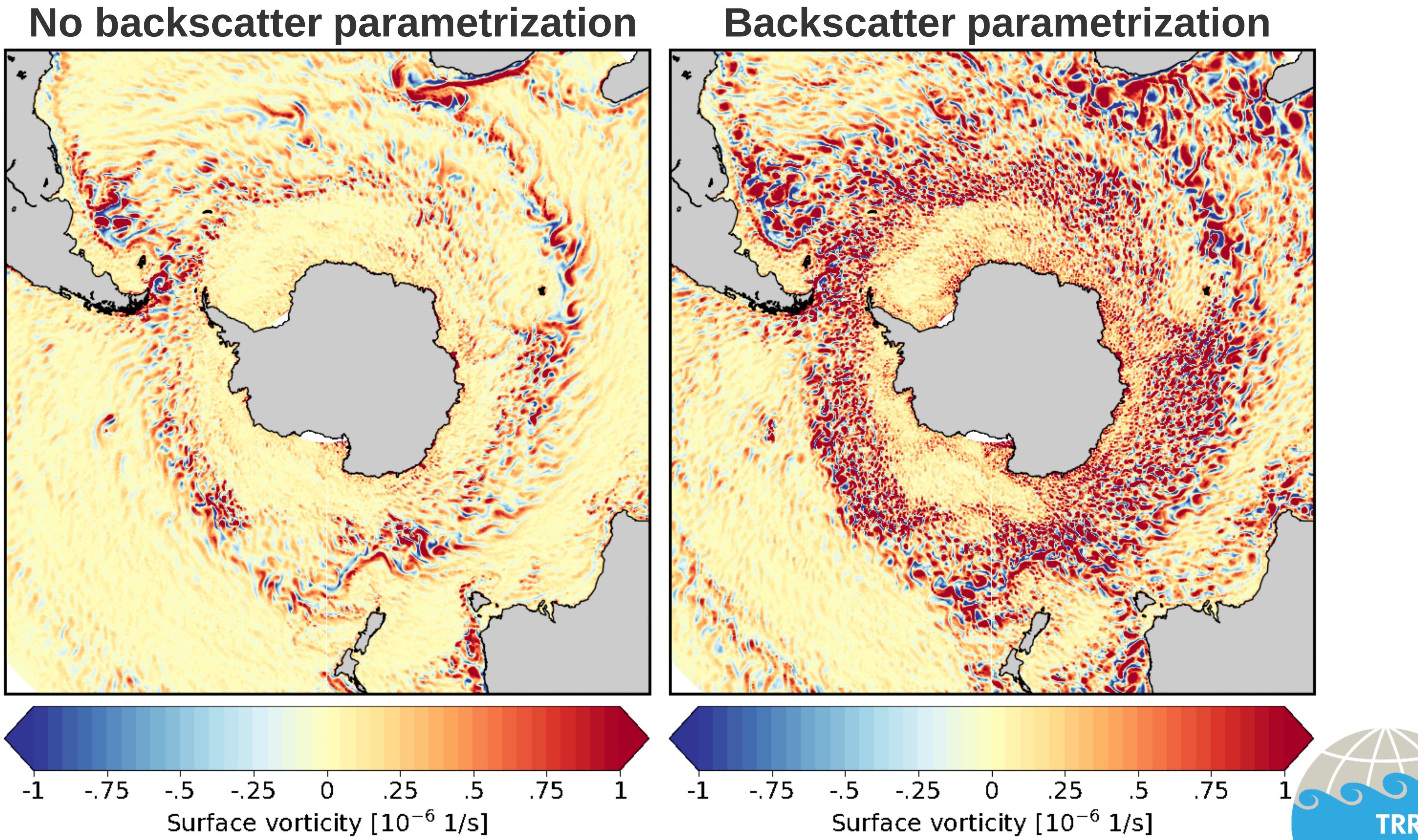
No backscatter parametrization
Backscatter parametrization
-1 -.75 -.5 -.25 0 .25 .5 .75 1
Surface vorticity [10⁻⁶ 1/s]
-1 -.75 -.5 -.25 0 .25 .5 .75 1
Surface vorticity [10⁻⁶ 1/s]

Sea surface height variability

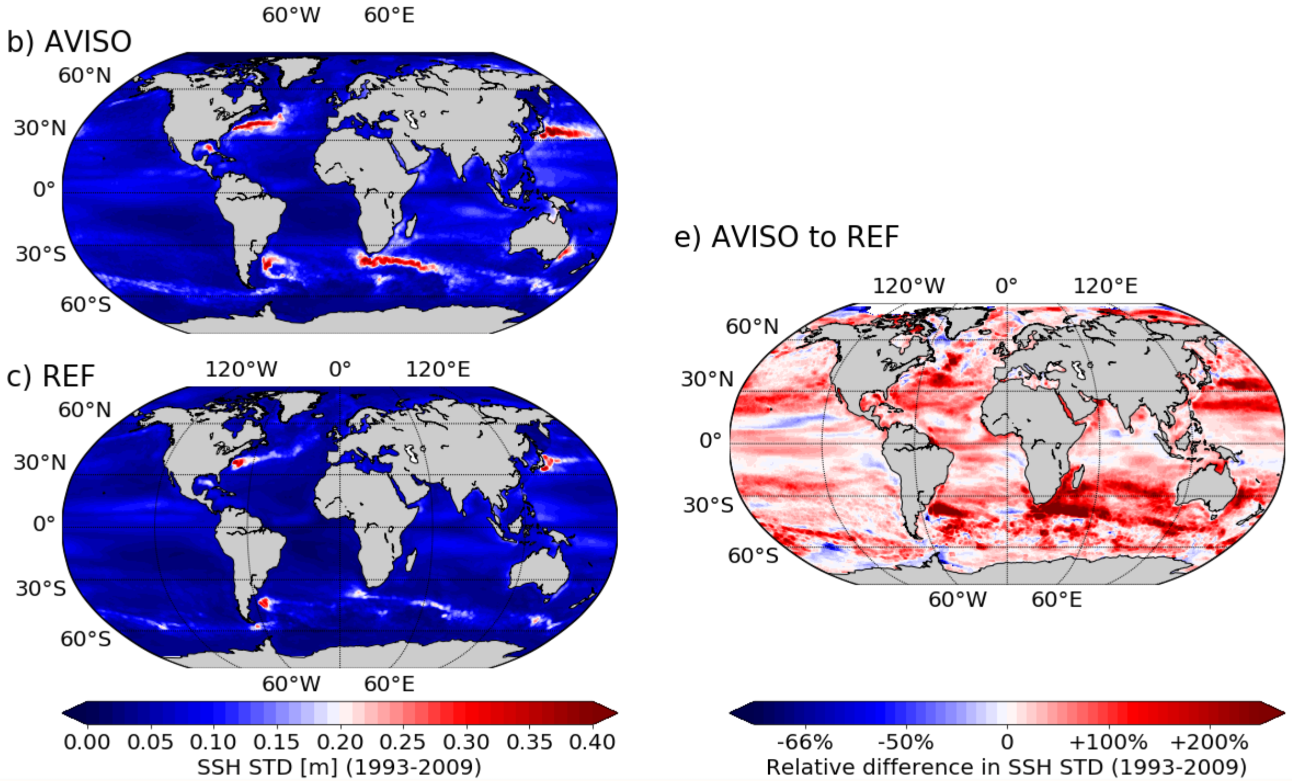

Sea surface height variability

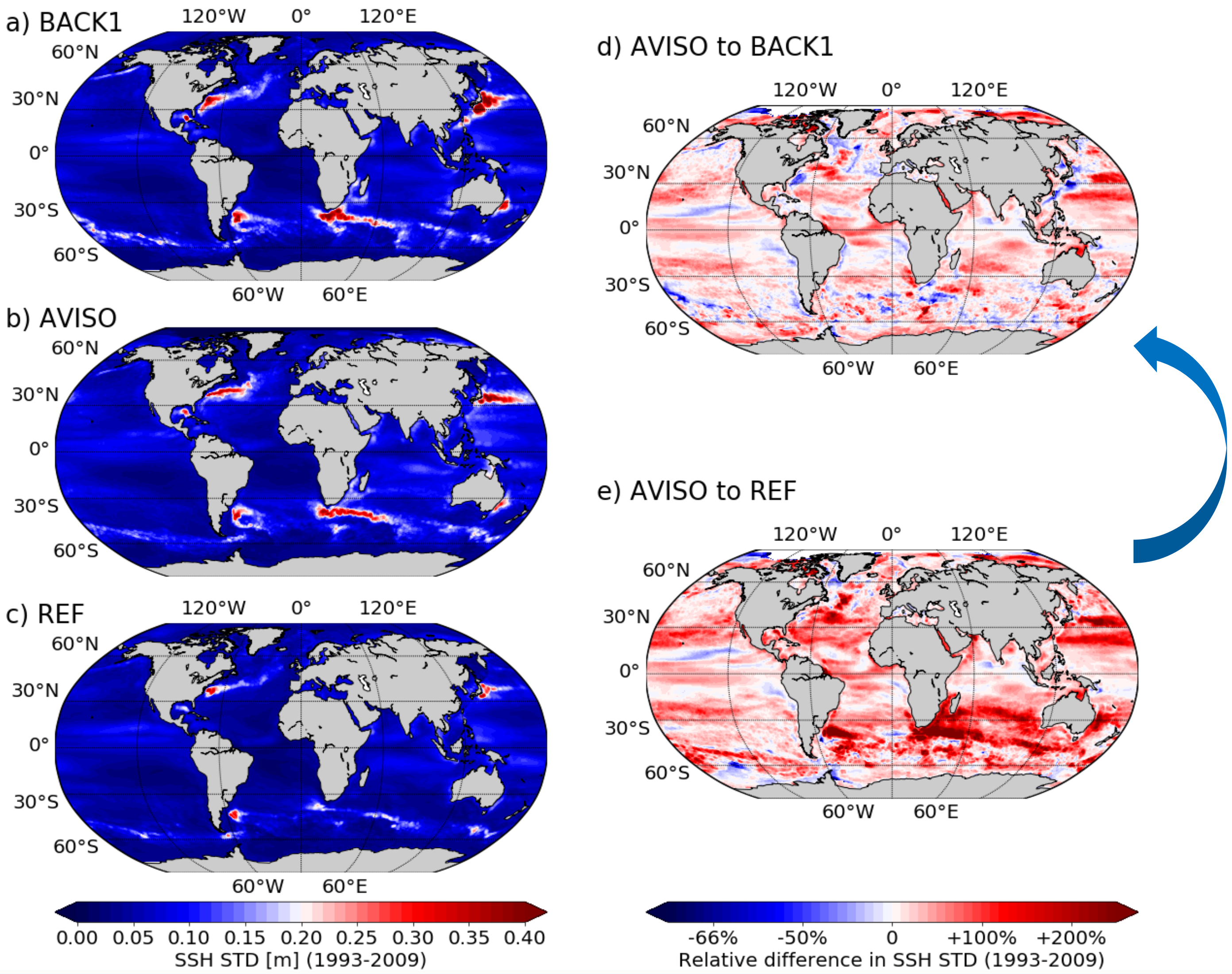

Velocity snapshots

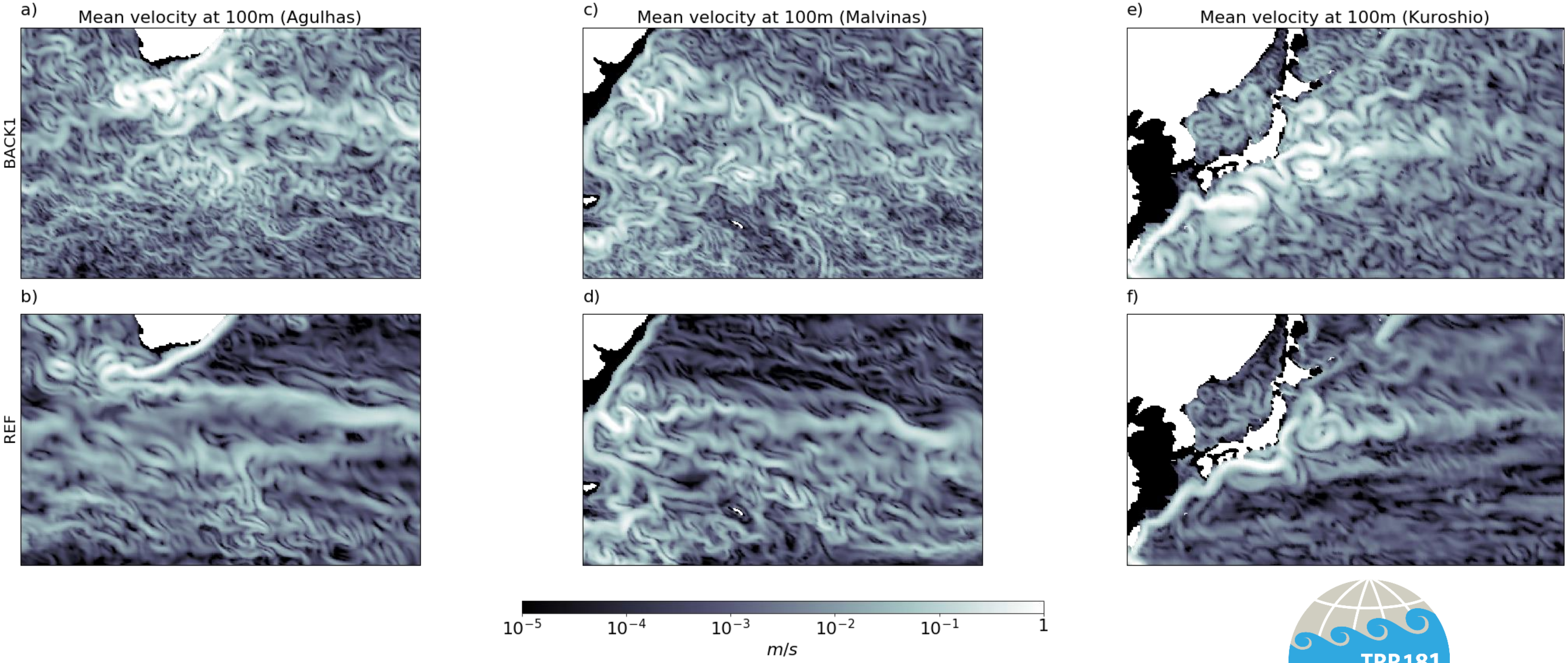

Mean SSH

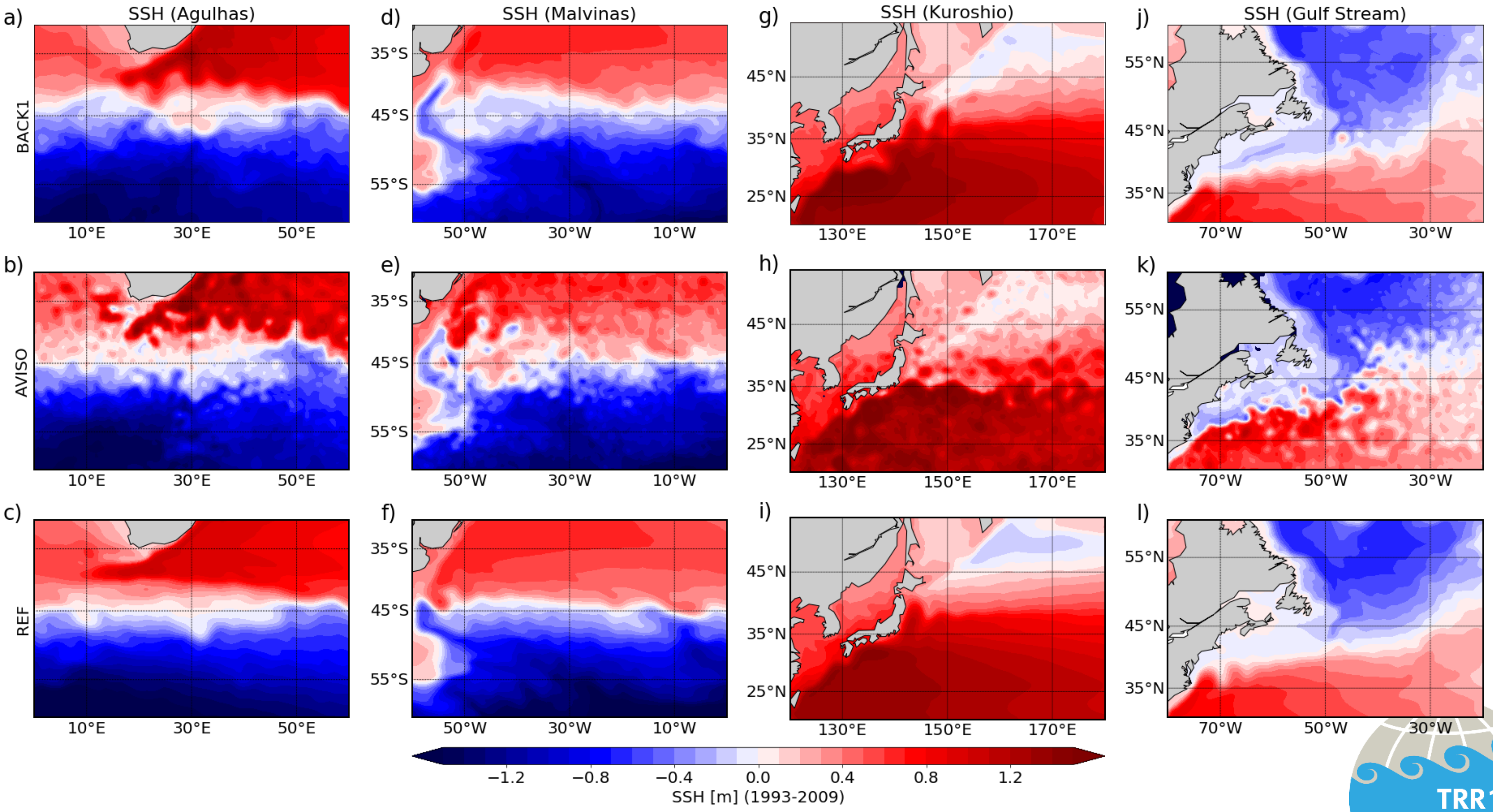
a)
SSH (Agulhas)
d)
SSH (Malvinas)
g)
SSH (Kuroshio)
j)
SSH (Gulf Stream)
BACK1
AVISO
REF
b)
e)
h)
k)
c)
f)
i)
l)
35°S
45°S
55°S
45°N
35°N
25°N
55°N
10°E
30°E
50°E
50°W
30°W
10°W
130°E
150°E
170°E
70°W
−1.2
−0.8
−0.4
0.0
0.4
0.8
1.2
SSH [m] (1993-2009)

Temperature bias

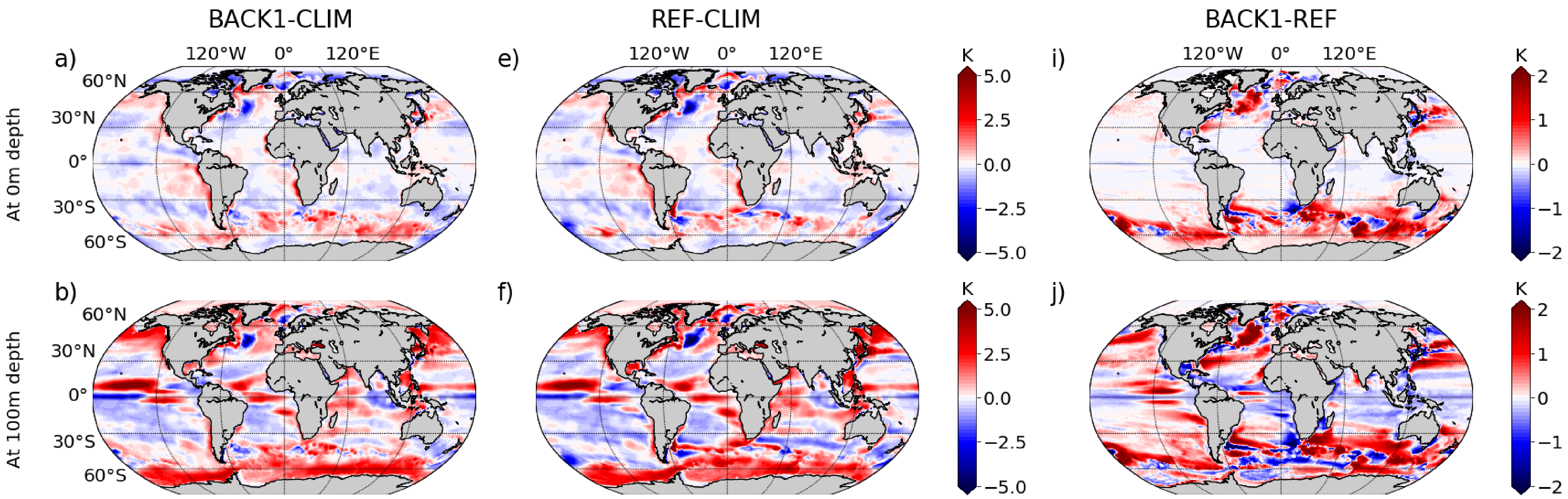

Temperature bias

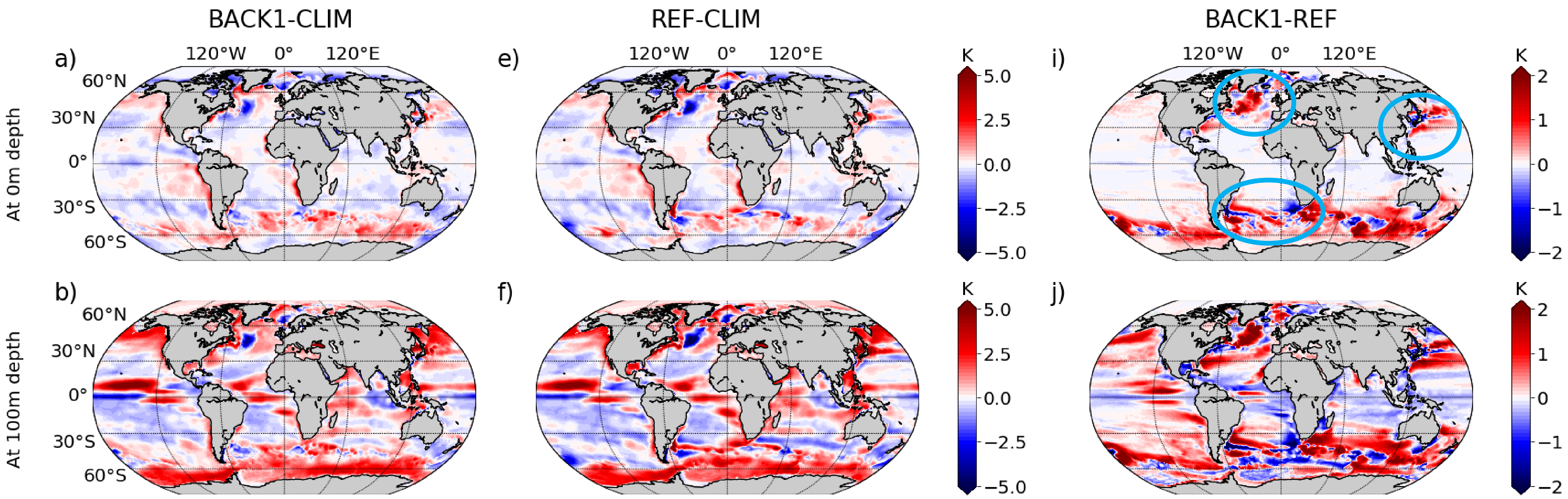

Temperature bias

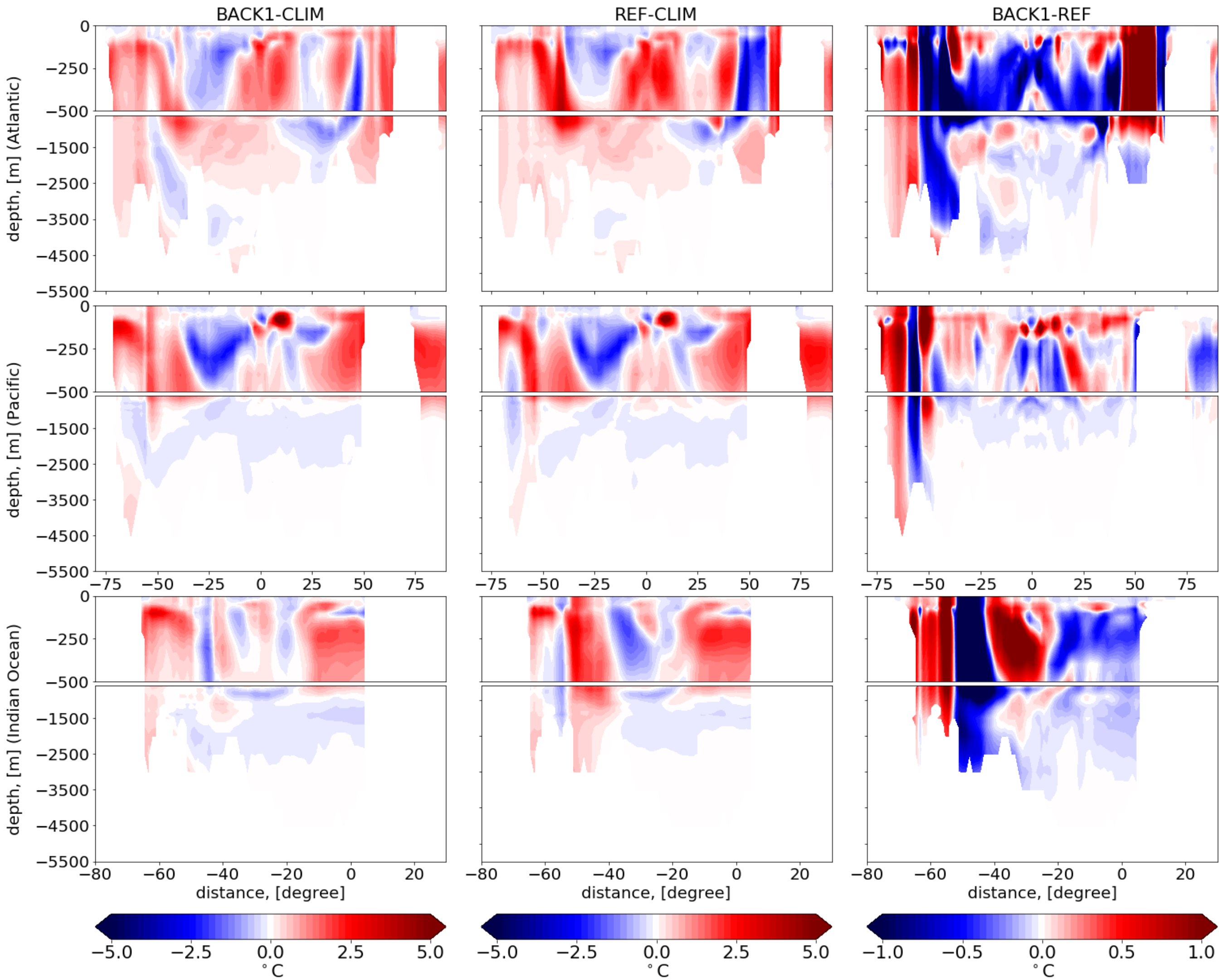

Temperature bias

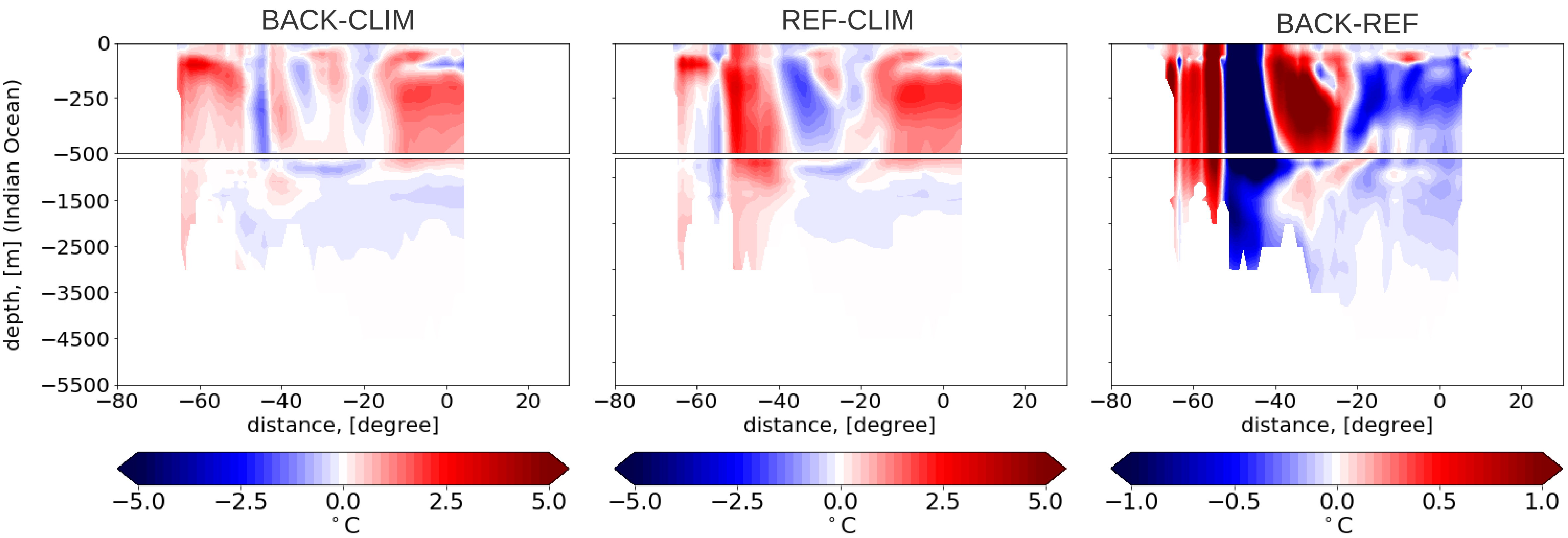

RMSE ratios BACK/REF

Region	SSH mean bias ratio	SSH std bias ratio
Global	0.894	0.925
Southern Ocean (30-60°S)	0.862	0.664
Agulhas (30-60°S, 0-60°E)	0.787	0.583
Malvinas (30-60°S, 60-0°W)	0.848	0.538
Kuroshio (20-50°N, 120-180°E)	1.075	1.007
Gulf Stream (30-60°N, 80-20°W)	0.992	0.949
30-60°S, 60-120°W	0.888	0.610
	T mean bias ratio	**S mean bias ratio**
Global surface	0.893	0.875
Global 100m	0.948	0.998
Global 1000m	0.998	1.000
Global 2000m	0.985	1.000
Atlantic transect	0.777	0.867
Pacific transect	0.960	0.889
Indian transect	0.685	0.716

TRR181

RMSE ratios BACK/REF

Region	SSH mean bias ratio	SSH std bias ratio
Global	0.894	0.925
Southern Ocean (30-60°S)	0.862	0.664
Agulhas (30-60°S, 0-60°E)	0.787	0.583
Malvinas (30-60°S, 60-0°W)	0.848	0.538
Kuroshio (20-50°N, 120-180°E)	1.075	1.007
Gulf Stream (30-60°N, 80-20°W)	0.992	0.949
30-60°S, 60-120°W	0.888	0.610
	T mean bias ratio	S mean bias ratio
Global surface	0.893	0.875
Global 100m	0.948	0.998
Global 1000m	0.998	1.000
Global 2000m	0.985	1.000
Atlantic transect	0.777	0.867
Pacific transect	0.960	0.889
Indian transect	0.685	0.716

Sea ice

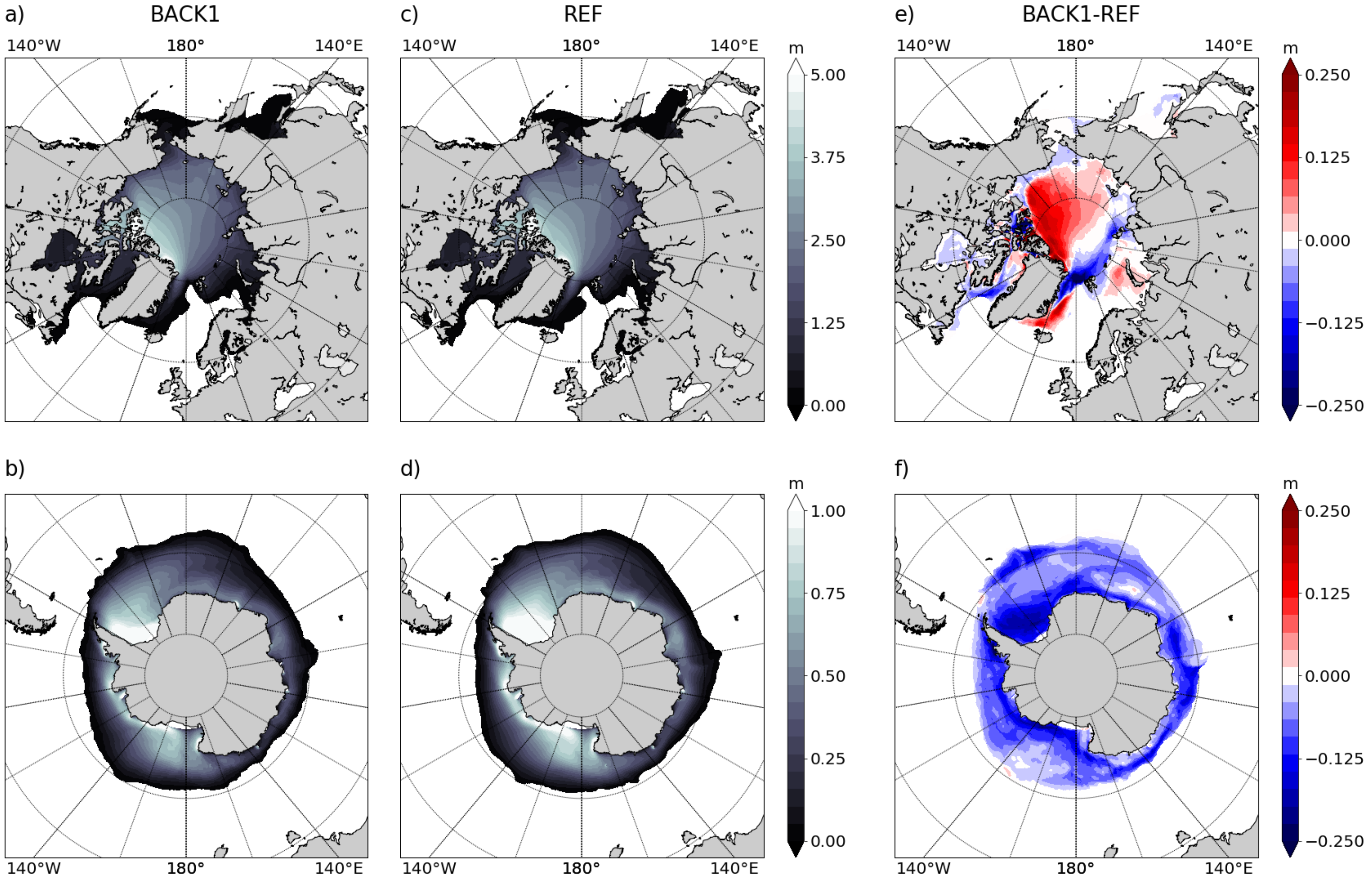
a)
BACK1
c)
REF
e)
BACK1-REF
b)
d)
f)
140°W
180°
140°E
m
5.00
3.75
2.50
1.25
0.00
1.00
0.75
0.50
0.25
0.250
0.125
0.000
−0.125
−0.250

Subgrid energy

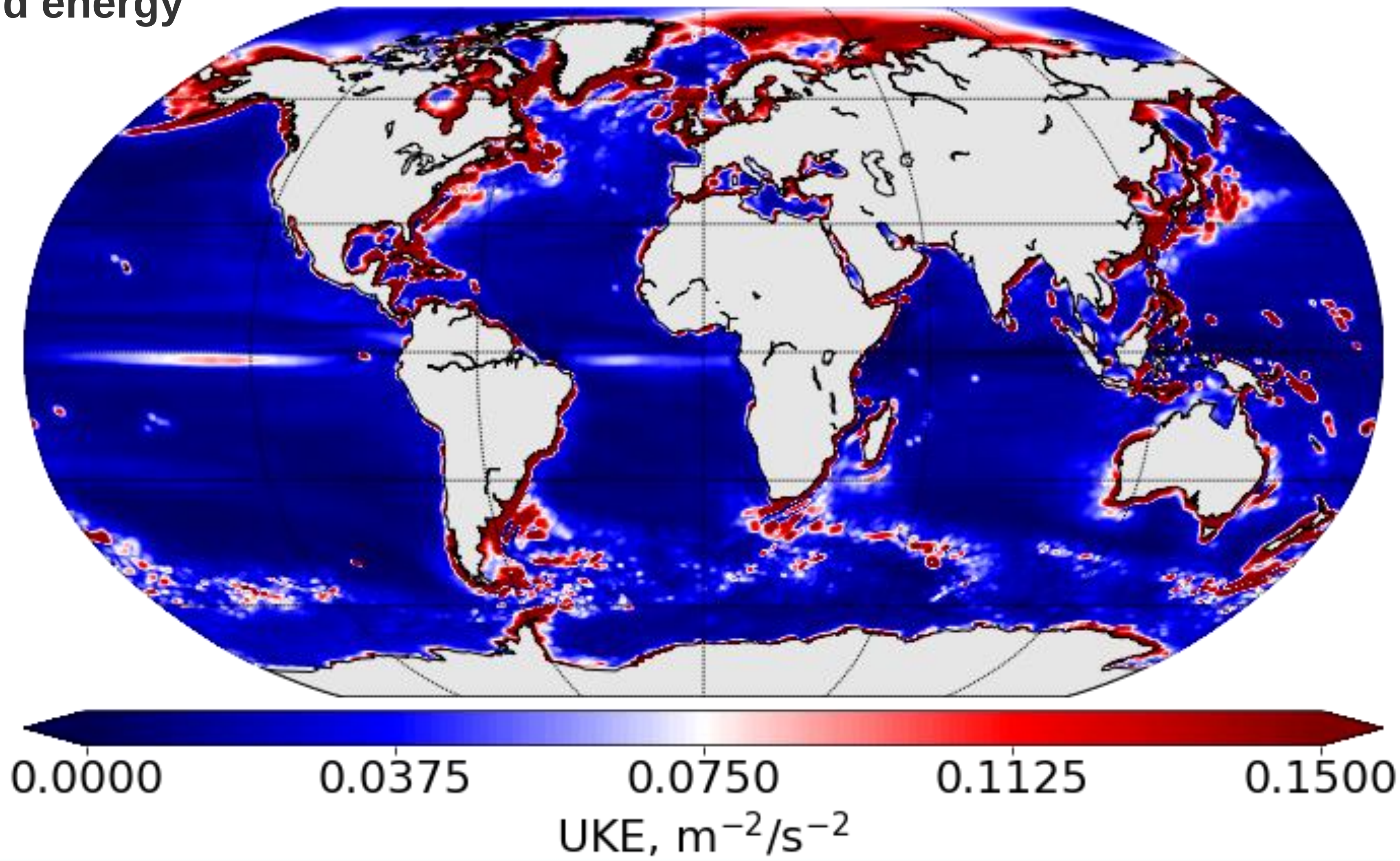

OUTLOOK

Improvement of parametrization of physical dissipation (reduction of timestep)

Use different resolutions and compare costs and quality of simulations

Different versions of backscatter, e.g. simplified, instantaneous backscatter; investigation of new combined operators

Extended diagnostics in the framework of effective resolution, dissipation vs. forcing scales, effects of operator choices

Idealized setups for intercomparison of different schemes, models (FESOM vs ICON), etc.

Extension to non eddy-resolving grids (inclusion of GM eddy parametrization)

CONCLUSIONS

Backscatter leads to strongly reduced energy dissipation and a more realistic total kinetic energy comparable to higher resolution simulations

Additional costs for backscatter scheme around 50% (channel) to 150% (global) while costs for resolution increase are more than (channel) or around (global) an order of magnitude

Improves variability as well as mean flow (with some exceptions) not only for velocity and SSH but also temperature and salinity

Juricke, S., S. Danilov, A. Kutsenko, M. Oliver, 2019: Ocean kinetic energy backscatter parametrizations on unstructured grids: Impact on mesoscale turbulence in a channel. *Ocean Modelling*, 138, 51-67

Juricke, S., S. Danilov, N. Koldunov, M. Oliver, D. Sidorenko, 2020: Ocean kinetic energy backscatter parametrization on unstructured grids: Impact on global eddy-permitting simulations. *Journal of Advances in Modeling Earth Systems*, 12, e2019MS001855.

sjuricke@awi.de